JOURNAL OF MATERIALS SCIENCE 31 (1996) 2221–2226

The influence of diffusion of carbon in ferrite as well as in austenite on a model of reaustenitization from ferrite/cementite mixtures in Fe–C steels

T. AKBAY
Department of Materials, Imperial College of Science, Technology and Medicine, Prince Consort Road, London SW7 2BP, UK

C. ATKINSON
Department of Mathematics, Imperial College of Science, Technology and Medicine, 180 Queen's Gate, London SW7 2RH, UK

The kinetics of formation of austenite from ferrite and cementite mixtures has been modelled by assuming the local equilibrium at the planar phase interfaces. The exact solutions to the diffusion equations governing the volume diffusion of carbon in austenite and ferrite are presented. The concurrent motions of the two interfaces are calculated via solving a set of transcendental equations derived from the flux balance conditions. At low isothermal transformation temperatures, it is found that the time required for reaustenitization is slightly greater than the time previously calculated with no diffusion of carbon in ferrite.

1. Introduction

The experimental work on the kinetics of austenite formation predates much of the attention on the kinetics of austenite decomposition (forward transformation). Hultgren [1] analysed isothermal growth of austenite and disappearance of ferrite in considerable detail. His method was later used by Davenport and Bain in determining the time–temperature–transformation (TTT) diagrams for steels [2]. Roberts and Mehl [3], in addition to the review of the work prior to 1940, reported a study of austenite formation from ferrite/pearlite and ferrite/spheroidite.

Kinetics of the nucleation and growth of austenite are a strong function of starting microstructure and alloy composition [3–7]. For ferrite/cementite mixtures (e.g. heavily tempered martensite, spheroidized pearlite) being the starting microstructure which is of interest to us here, austenite first forms at ferrite/cementite interfaces [8]. In particular, when the average carbon content is low, austenite rapidly envelops spherical cementite particles, so that the geometry becomes spherically symmetrical.

The reader should note that the form of the time–temperature–transformation (TTT) diagram for reaustenitization is different from the classical *C*-curve describing the forward transformation, i.e. when austenite decomposes to allotriomorphic ferrite, pearlite, bainite etc. Since both the driving force and the diffusion coefficient increase with increasing temperature, the TTT diagram for reaustenitization has the form of a half-*C* [9–12], so that the time required for reverse transformation decreases monotonically with increasing temperature.

Theoretical analyses [3, 8, 13] of the rate of formation of austenite from various aggregates of ferrite and cementite usually assume that the rate controlling step is the diffusion of carbon through austenite. As was recognised by Hultgren in 1929 [1], the growth of austenite requires the simultaneous movement of two interphase boundaries: the θ/γ as well as the γ/α interface (see Fig. 1). The models emphasize the importance of cementite precipitates in aiding the nucleation of austenite. Hillert [13] identified distinct regimes for the process of reaustenitization from ferrite/cementite aggregates, the applicability of each depending upon cementite particle size and spacing, temperature and alloy composition. In particular, when the distance between particles of cementite is very large (i.e. when the mean carbon content is low), the cementite particles rapidly become engulfed by austenite, after which time further growth of austenite is controlled by carbon diffusion in the austenite shell. In all cases considered so far, full chemical equilibrium in the close vicinity of the moving interfaces (the local equilibrium hypothesis) has been applied with strong experimental support.

In most of the early work, the Laplacian form of the diffusion field of the diffusing species in austenite, i.e. the steady state assumption, was applied [3, 13]. Recently, Akbay *et al.* [14] presented analytical and

0022–2461

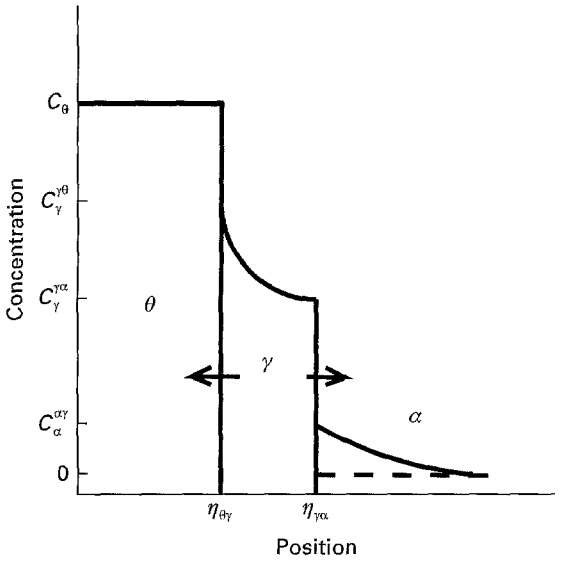

Figure 1. Schematic diagram of interstitial solute concentration profiles. Dashed line represents the constant value employed in the previous analysis in which no diffusion of carbon in α was considered.

numerical solutions to the transient problem which revealed the fact that the steady state analysis is only true at low isothermal transformation temperatures. As part of a systematic developement of reaustenitization models, it is reasonable to investigate the effect of diffusion of carbon in ferrite in addition to austenite on the overall efficiency of the model. The diffusion equations are solved in ferrite and austenite (the growing phase) subject to flux balance conditions at the θ/γ and γ/α boundaries.

2. Mathematical description of the problem

In order to model reaustenitization from ferrite/cementite mixtures, it is necessary to simulate the austenite nucleation event by introducing a thin layer of austenite at the ferrite/cementite boundary. The following additional simplifying assumptions are made in the present work.

(i) Local equilibrium is assumed to apply at the cementite/austenite (θ/γ) and austenite/ferrite (γ/α) phase boundaries;
(ii) the Fe–C binary system is considered, to avoid the complexity due to the diffusion of substitutional solutes;
(iii) the diffusion of carbon in cementite is ignored, since cementite is near stoichiometric;
(iv) the concentration dependence of the diffusivity of carbon in austenite is taken into account by employing a weighted average value. A more elaborate analysis, by the authors, taking the full concentration dependence into account can be found elsewhere [15].

Under these assumptions, the process is controlled by the diffusion of carbon in austenite and ferrite. The variation of C_γ, the carbon concentration in austenite, with time t and distance r (measured outward from the centre of the cementite block) is given by

$$\frac{\partial C_\gamma}{\partial t} = \frac{\bar{D}_C^\gamma}{r^n}\frac{\partial}{\partial r}\left(r^n\frac{\partial C_\gamma}{\partial r}\right) \quad (1)$$

where $\bar{D}_C^\gamma$ is the weighted average diffusivity of carbon in austenite and n is an integer which takes a value of 0 for planar, 1 for cylindrical, 2 for spherical geometries respectively. Similarly, the variation of C_α, the carbon concentration in ferrite, with time t and distance r, satisfies

$$\frac{\partial C_\alpha}{\partial t} = \frac{\bar{D}_C^\alpha}{r^n}\frac{\partial}{\partial r}\left(r^n\frac{\partial C_\alpha}{\partial r}\right) \quad (2)$$

where $\bar{D}_C^\alpha$ is the diffusivity of carbon in ferrite.

The flux balance condition at the θ/γ interface is given by

$$(C_\theta - C_\gamma^{\gamma\theta})\frac{dr_{\theta\gamma}}{dt} = \bar{D}_C^\gamma\left(\frac{\partial C_\gamma}{\partial r}\right)_{r=r_{\theta\gamma}^+} \quad (3)$$

and at the γ/α interface by

$$(C_\gamma^{\gamma\alpha} - C_\alpha^{\alpha\gamma})\frac{dr_{\gamma\alpha}}{dt} = -\bar{D}_C^\gamma\left(\frac{\partial C_\gamma}{\partial r}\right)_{r=r_{\gamma\alpha}^-} + \bar{D}_C^\alpha\left(\frac{\partial C_\alpha}{\partial r}\right)_{r=r_{\gamma\alpha}^+} \quad (4)$$

where $r_{\theta\gamma}\{t\}$ and $r_{\gamma\alpha}\{t\}$ are the instantaneous positions of the θ/γ and γ/α interfaces respectively. The terms $C_\gamma^{\gamma\theta}$ and $C_\gamma^{\gamma\alpha}$ represent the concentrations of carbon in austenite at the γ/θ and γ/α interfaces. Also the term $C_\alpha^{\alpha\gamma}$ denotes the carbon concentration in ferrite at the γ/α interface. The initial boundary conditions are expressed by

$$r_{\theta\gamma} = r_0 \quad (5)$$

$$r_{\gamma\alpha} = r_0 \quad (6)$$

and

$$C = C_\theta \quad \text{for} \quad 0 \leqslant r \leqslant r_0 \quad (7)$$

where r_0 is the initial size of the cementite block. Local equilibrium at the θ/γ and γ/α interfaces implies

$$C_\gamma = C_\gamma^{\gamma\theta} \quad \text{at } r = r_{\theta\gamma}^+ \quad (8)$$

$$C_\gamma = C_\gamma^{\gamma\alpha} \quad \text{at } r = r_{\gamma\alpha}^- \quad (9)$$

$$C_\alpha = C_\alpha^{\alpha\gamma} \quad \text{at } r = r_{\gamma\alpha}^+ \quad (10)$$

$$C_\alpha = 0 \text{ at } r = +\infty \quad (11)$$

In this work, we show that it is possible to obtain exact solutions to Equations 1 and 2 subject to 3–11 for the case $n = 0$ (i.e. planar geometry).

2.1 Exact solutions

For planar geometry, Boltzmann's transformation $\eta = (r - r_0)(D_0 t)^{-1/2}$, where D_0 is a normalization constant and r_0 is the initial size of the cementite particle, reduces Equation 1 to an ordinary differential equation of the form

$$-\frac{\eta}{2}\frac{dC_\gamma}{d\eta} = D_C^\gamma\frac{d^2C_\gamma}{d\eta^2} \quad (12)$$

where $D_C^\gamma = \bar{D}_C^\gamma/D_0$. In addition, Equation 2 will be transformed as

$$-\frac{\eta}{2}\frac{dC_\alpha}{d\eta} = D_C^\alpha\frac{d^2C_\alpha}{d\eta^2} \quad (13)$$

where $D_C^\alpha = \bar{D}_C^\alpha / D_0$. Similarly the flux balance conditions 3 and 4 are transformed into

$$(C_\theta - C_\gamma^{\gamma\theta})\frac{\eta_{\theta\gamma}}{2} = D_C^\gamma \left(\frac{dC_\gamma}{d\eta}\right)_{\eta=\eta_{\theta\gamma}^+} \quad (14)$$

$$(C_\gamma^{\gamma\alpha} - C_\alpha^{\alpha\gamma})\frac{\eta_{\gamma\alpha}}{2} = -D_C^\gamma \left(\frac{dC_\gamma}{\partial\eta}\right)_{\eta=\eta_{\gamma\alpha}^-} + D_C^\alpha \left(\frac{dC_\alpha}{d\eta}\right)_{\eta=\eta_{\gamma\alpha}^+} \quad (15)$$

The solution of Equation 12 can be written as

$$C_\gamma = A\int_{\eta_{\theta\gamma}}^{\eta} \exp\left\{-\frac{\eta^2}{4D_C^\gamma}\right\}d\eta + B \quad (16)$$

where the constants A and B are found by applying the boundary conditions 8 and 9 to give

$$A = \frac{(C_\gamma^{\gamma\alpha} - C_\gamma^{\gamma\theta})}{\int_{\eta_{\theta\gamma}}^{\eta_{\gamma\alpha}} \exp\left\{-\frac{\eta^2}{4D_C^\gamma}\right\}d\eta}, \quad B = C_\gamma^{\gamma\theta} \quad (17)$$

Similarly the solution to Equation 13 will be

$$C_\alpha = E\int_{\eta_{\gamma\alpha}}^{\eta} \exp\left\{-\frac{\eta^2}{4D_C^\alpha}\right\}d\eta + F \quad (18)$$

where the constants E and F are found by applying the boundary conditions 10 and 11 to give

$$E = \frac{C_\alpha^{\alpha\gamma}}{\int_{\eta_{\gamma\alpha}}^{+\infty} \exp\left\{-\frac{\eta^2}{4D_C^\alpha}\right\}d\eta}, \quad F = C_\alpha^{\alpha\gamma} \quad (19)$$

The interface flux balance conditions 14 and 15 can now be written as

$$(C_\theta - C_\gamma^{\gamma\theta})\frac{\eta_{\theta\gamma}}{2} = \frac{D_C^\gamma (C_\gamma^{\gamma\alpha} - C_\gamma^{\gamma\theta})}{\int_{\eta_{\theta\gamma}}^{\eta_{\gamma\alpha}} \exp\left\{-\frac{\eta^2}{4D_C^\gamma}\right\}d\eta} \exp\left\{\frac{-\eta_{\theta\gamma}^2}{4D_C^\gamma}\right\} \quad (20)$$

$$(C_\gamma^{\gamma\alpha} - C_\alpha^{\alpha\gamma})\frac{\eta_{\gamma\alpha}}{2} = -\frac{D_C^\gamma (C_\gamma^{\gamma\alpha} - C_\gamma^{\gamma\theta})}{\int_{\eta_{\theta\gamma}}^{\eta_{\gamma\alpha}} \exp\left\{-\frac{\eta^2}{4D_C^\gamma}\right\}d\eta} \exp\left\{\frac{-\eta_{\gamma\alpha}^2}{4D_C^\gamma}\right\} - \frac{D_C^\alpha C_\alpha^{\alpha\gamma}}{\int_{\eta_{\gamma\alpha}}^{+\infty} \exp\left\{-\frac{\eta^2}{4D_C^\alpha}\right\}d\eta} \exp\left\{\frac{-\eta_{\gamma\alpha}^2}{4D_C^\alpha}\right\} \quad (21)$$

Using the definition of the error function $\mathrm{erf}\{\phi\} = 2/(\pi)^{1/2}\int_0^\phi \exp\{-\xi^2\}\,d\xi$, Equations 20 and 21 can be rearranged to yield

$$(C_\theta - C_\gamma^{\gamma\theta})\eta_{\theta\gamma} = \left(\frac{4D_C^\gamma}{\pi}\right)^{1/2} \frac{(C_\gamma^{\gamma\alpha} - C_\gamma^{\gamma\theta})}{\left[\mathrm{erfc}\left\{\frac{\eta_{\theta\gamma}}{2(D_C^\gamma)^{1/2}}\right\} - \mathrm{erfc}\left\{\frac{\eta_{\gamma\alpha}}{2(D_C^\gamma)^{1/2}}\right\}\right]} \exp\left\{-\frac{\eta_{\theta\gamma}^2}{4D_C^\gamma}\right\} \quad (22)$$

$$(C_\gamma^{\gamma\alpha} - C_\alpha^{\alpha\gamma})\eta_{\gamma\alpha} = -\left(\frac{4D_C^\gamma}{\pi}\right)^{1/2} \frac{(C_\gamma^{\gamma\alpha} - C_\gamma^{\gamma\theta})}{\left[\mathrm{erfc}\left\{\frac{\eta_{\theta\gamma}}{2(D_C^\gamma)^{1/2}}\right\} - \mathrm{erfc}\left\{\frac{\eta_{\gamma\alpha}}{2(D_C^\gamma)^{1/2}}\right\}\right]} \exp\left\{-\frac{\eta_{\gamma\alpha}^2}{4D_C^\gamma}\right\}$$

$$-\left(\frac{4D_C^\alpha}{\pi}\right)^{1/2} \frac{C_\alpha^{\alpha\gamma}}{\mathrm{erfc}\left\{\frac{\eta_{\gamma\alpha}}{2(D_C^\alpha)^{1/2}}\right\}} \exp\left\{-\frac{\eta_{\gamma\alpha}^2}{4D_C^\alpha}\right\} \quad (23)$$

The positions of the interfaces can be obtained by simultaneous solution of the coupled transcendental Equations 22 and 23 for dimensionless interface parameters $\eta_{\theta\gamma}$ and $\eta_{\gamma\alpha}$.

2.2 Limiting case

In this section the authors wish to investigate the consequences of the competition between solute diffusion in γ and α. It should be pointed out that under favourable conditions the fluxes of the diffusing species across the interface may balance preventing it from being migrated. In order to assess the viability of this phenomenon for the Fe–C binary system the following mathematical analysis will be performed.

Suppose the dimensionless parameter for γ/α interface, $\eta_{\gamma\alpha}$, is identically zero then it is clear that one can reduce the Equation 23 into the following form.

$$-\left(\frac{4D_C^\gamma}{\pi}\right)^{1/2} \frac{(C_\gamma^{\gamma\alpha} - C_\gamma^{\gamma\theta})}{\left[\mathrm{erfc}\left\{\frac{\eta_{\theta\gamma}}{2(D_C^\gamma)^{1/2}}\right\} - 1\right]} = \left(\frac{4D_C^\alpha}{\pi}\right)^{1/2} C_\alpha^{\alpha\gamma} \quad (24)$$

Substituting the above equation into Equation 22 yields

$$(C_\theta - C_\gamma^{\gamma\theta})\eta_{\theta\gamma} = -\left(\frac{4D_C^\alpha}{\pi}\right)^{1/2} C_\alpha^{\alpha\gamma} \exp\left\{-\frac{\eta_{\theta\gamma}^2}{4D_C^\gamma}\right\} \quad (25)$$

Now a new variable, $\bar{\eta}_{\theta\gamma}$, may be defined as equal to $\eta_{\theta\gamma}/(D_C^{\gamma})^{1/2}$ to rewrite Equations 24 and 25 as

$$-(C_\gamma^{\gamma\alpha} - C_\gamma^{\gamma\theta}) = \left(\frac{D_C^{\alpha}}{D_C^{\gamma}}\right)^{1/2} C_\alpha^{\alpha\gamma}\left[\operatorname{erfc}\left\{\frac{\bar{\eta}_{\theta\gamma}}{2}\right\} - 1\right] \quad (26)$$

$$(C_\theta - C_\gamma^{\gamma\theta})\bar{\eta}_{\theta\gamma} = -\left(\frac{4D_C^{\alpha}}{\pi D_C^{\gamma}}\right)^{1/2} C_\alpha^{\alpha\gamma}\exp\left\{-\frac{\bar{\eta}_{\theta\gamma}^2}{4}\right\} \quad (27)$$

Hence the interface parameter $\bar{\eta}_{\theta\gamma}$ and the ratio of carbon diffusivity in ferrite to that in austenite, $D_C^{\alpha}/D_C^{\gamma}$, can be calculated by simultaneously solving the Equations 26 and 27. The solution will provide the required magnitude of $D_C^{\alpha}/D_C^{\gamma}$ to stop the migration of the γ/α interface.

3. Results and discussion

The results of the theory developed in the previous sections will be illustrated here. The equilibrium interstitial solute concentrations corresponding to the $\alpha/(\alpha+\gamma)$, $(\alpha+\gamma)/\gamma$ and $\gamma/(\gamma+\theta)$ phase boundaries for the Fe–C binary system are calculated by the numerical minimization of Gibbs energy using the sublattice model [16, 17] with associated data [18]. Equations 22 and 23 can be solved for a pair of dimensionless parameters, $\eta_{\theta\gamma}$ and $\eta_{\gamma\alpha}$ by specifying the transformation temperature which in turn dictates the local equilibrium concentrations at the interfaces. Mole fractions are chosen for the carbon concentrations in the phases considered.

The constant for the diffusivity of carbon in austenite ($\bar{D}_C^{\gamma}$) is evaluated taking the weighted averages of the concentration dependent ones. The numerical evaluation as a function of concentration and temperature follows Bhadeshia's method [19] based on references [20, 21]. On the other hand, the method proposed by McLellan *et al.* [22, 23] is adopted for the calculation of the diffusion coefficient of carbon in ferrite. Table I lists the calculated values of $\bar{D}_C^{\alpha}$ and $\bar{D}_C^{\gamma}$ for various transformation temperatures.

Figs 2 and 3 illustrate the variation of dimensionless interface parameters, $\eta_{\theta\gamma}$ and $\eta_{\gamma\alpha}$, against isothermal transformation temperatures. Some discussion is warranted concerning the difference between the two calculations with or without employing the carbon diffusion in α. The solid lines are the results of the analysis for which the carbon diffusion in α is ignored. The retardation of the migration of the γ/α interface due to relatively slower rearrangement of carbon atoms inside the α region compared to non-diffusion case is observed. This in turn causes an acceleration of the θ/γ interface due to rapid carbon rejection from the θ into γ.

As was discussed earlier, it is possible to calculate the ratios of the diffusivities of carbon in α to that in γ. It is particularly important to consider a limiting case at which the γ/α interface may have ceased to move. Typical values of the calculated ratio via solving the Equations 26 and 27 are tabulated in Table II. It must be stressed that the actual values of $\bar{D}_C^{\alpha}/\bar{D}_C^{\gamma}$ can never

TABLE I Calculated diffusivities of carbon in α and γ.

Temperature °C	$\bar{D}_C^{\alpha}$ ($m^2 s^{-1}$) $\times 10^{-10}$	$\bar{D}_C^{\gamma}$ ($m^2 s^{-1}$) $\times 10^{-12}$
730	1.2768	1.0850
750	1.5762	1.4469
800	2.5797	2.9904
850	4.0422	6.1155
900	6.0978	12.251

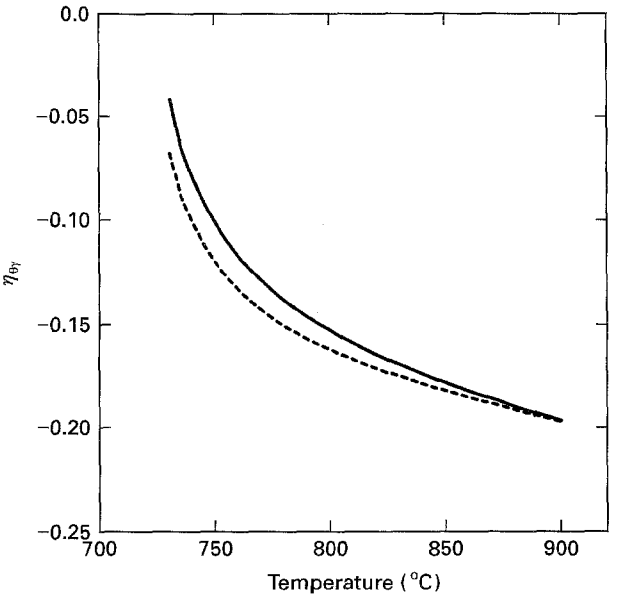

Figure 2. The variation of the θ/γ interface parameter $\eta_{\theta\gamma}$ with isothermal transformation temperature for the Fe–C system. Planar geometry. Solid curve: with no diffusion of carbon in α. Dashed curve: with diffusion of carbon in α.

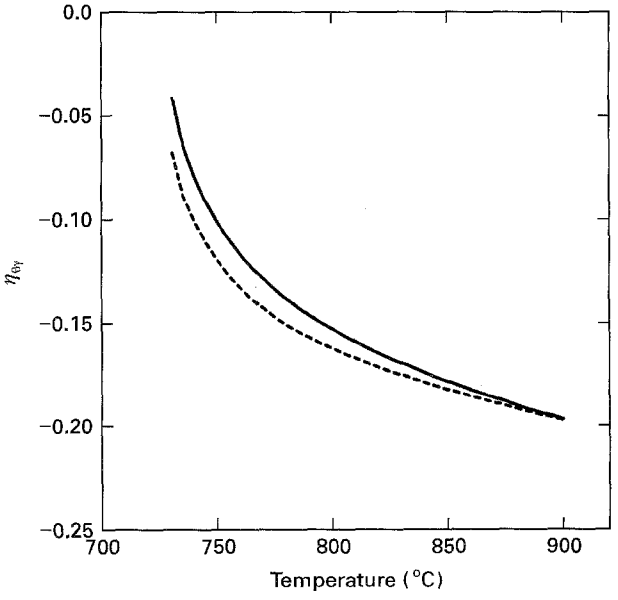

Figure 3. The variation of the γ/α interface parameter $\eta_{\gamma\alpha}$ with isothermal transformation temperature for the Fe–C system. Planar geometry. Solid curve: with no diffusion of carbon in α. Dashed curve: with diffusion of carbon in α.

TABLE II Calculated ratios of diffusivities of carbon in α to that in γ.

Temperature °C	$\bar{D}_C^{\alpha}/\bar{D}_C^{\gamma}$ ($m^2 s^{-1}$)
730	6.2940×10^2
750	5.4941×10^3
800	3.0795×10^4
850	1.4240×10^5
900	4.6907×10^6

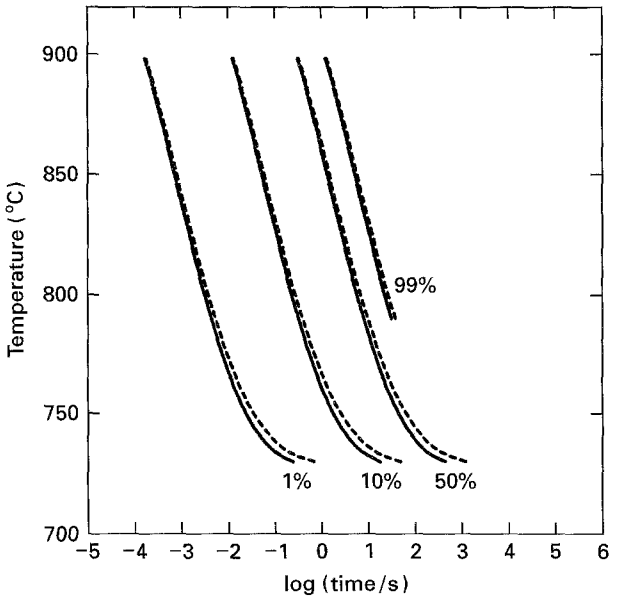

Figure 4. Reverse TTT diagram, Fe–0.4 wt % C steel, $r_0 = 1$ μm. Solid curve: with no diffusion of carbon in α. Dashed curve: with diffusion of carbon in α.

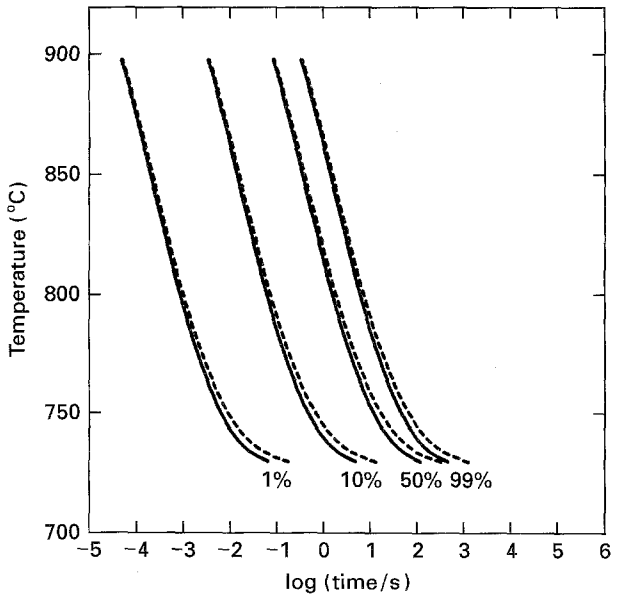

Figure 5. Reverse TTT diagram, Fe–0.8 wt % C steel, $r_0 = 1$ μm. Solid curve: with no diffusion of carbon in α. Dashed curve: with diffusion of carbon in α.

be as high as the ones that are calculated considering the limiting case.

Figs 4 and 5 depict the reverse TTT diagrams calculated for Fe–0.4 wt %C and Fe–0.8 wt %C binary steels considering the average θ particle size as 1 μm. The dashed curves represent various degrees of reaustenitization evaluated by the analysis presented here while the solid curves represent the case where diffusion of carbon in α is ignored. It should be emphasized that there is no great deal of difference between the two analyses at high temperatures but the one presented here predicts a slight delay in overall transformation kinetics for low temperatures.

4. Conclusion

The kinetics of formation of austenite from ferrite and cementite mixtures has been modelled. The local equilibrium at the phase interfaces was assumed. In addition, the process was assumed to be controlled by volume diffusion of carbon in both austenite and ferrite. The exact solutions to the diffusion equations governing the volume diffusion of carbon in austenite and ferrite were presented. The concurrent motions of the two interfaces were calculated via solving a set of transcendental equations derived from the flux balance conditions.

At low isothermal transformation temperatures, it was found that the time required for reaustenitization is slightly greater than the time previously calculated with no diffusion of carbon in ferrite. This is attributed to the higher magnitudes of the ratio of diffusivity of carbon in ferrite to that in austenite at low transformation temperatures. The diffusion of carbon allowed to occur in the ferritic region retards the motion of the γ/α interface while accelerating the θ/γ interface – the overall transformation rate being reduced.

Acknowledgements

Taner Akbay's contribution to this work was carried out under EPSRC grant GR/J 36938 'Theory for the Reaustenitisation Kinetics in Low Alloy Steels'. The authors acknowledge the assistance of Miss Kate Harris and Dr. Roger C. Reed. We are also grateful to Professor Malcolm McLean for the provision of research facilities at Imperial College.

References

1. A. HULTGREN, *Trans. Am. Soc. Steel Treat* **16** (1929) 227.
2. E. S. DAVENPORT and E. C. BAIN, *Trans. Am. Inst. Min. Engrs* **90** (1930) 117.
3. G. A. ROBERTS and R. F. MEHL, *Trans. Am. Soc. Metal* **31** (1943) 613.
4. G. R. SPEICH and A. SZIRMAE, *Metall. Trans.* **245** (1969) 1063.
5. C. I. GARCIA and A. J. DEARDO, *ibid.* **12A** (1981) 521.
6. G. R. SPEICH, V. A. DEMAREST and R. L. MILLER, *ibid.* **12A** (1981) 1419.
7. J. ÅGREN, *Scand. J. Metall.* **10** (1981) 134.
8. R. R. JUDD and H. W. PAXTON, *Trans. Metall. Soc. A.I.M.E.* **242** (1968) 206.
9. U.R. LENEL and R. W. K. HONEYCOMBE, Kinetics of the Formation of Austenite During Intercritical Annealing of a Low Alloy Steel, in *Advances in the Physical Metallurgy and Applications of Steels*, The Metals Society, (1981) pp. 38–46.
10. U. R. LENEL, *Scripta Metall.* **17** (1983) 471.
11. U. R. LENEL and R. W. K. HONEYCOMBE, *Metal Sci.* **18** (1984) 201.

12. *Idem, ibid.* **18** (1984) 503.
13. M. HILLERT, K. NILSSON and L.-E. TÖRNDAHL, *J. Iron Steel Inst.* **209** (1971) 49.
14. T. AKBAY, R. C. REED and C. ATKINSON, *Acta Metall. Mater.* **42** (1994) 1469.
15. C. ATKINSON and T. AKBAY, *ibid.* (1996) in print.
16. M. HILLERT and L.-I. STAFFANSON, *Acta Chem. Scand.* **24** (1970) 3618.
17. B. SUNDMAN and J. ÅGREN, *J. Phys. Chem. Solids* **42** (1981) 297.
18. P. GUSTAFSON, *Scan. J. Metall.* **14** (1985) 259.
19. H. K. D. H. BHADESHIA, *Metal Science* **15** (1981) 477.
20. R. H. SILLER and R. B. McLELLAN, *Trans. Metall. Soc. A.I.M.E.* **245** (1969) 697.
21. *Idem., Metall. Trans.* **1** (1970) 985.
22. R. B. McLELLAN, M. L. RUDEE and T. ISHIBACHI, *Trans. Metall. Soc. A.I.M.E.* **233** (1965) 1938.
23. R. B. McLELLAN and M. L. WASZ, *J. Phys. Chem. Solids* **54** (1993) 583.

Received 23 October 1995
and accepted 20 November 1995